

## ARTICLE

# Vibrational and Structural Dynamics of $\text{Mn}(\text{CO})_5\text{Br}$ and $\text{Re}(\text{CO})_5\text{Br}$ Examined Using Nonlinear Infrared Spectroscopy<sup>†</sup>

Min-jun Feng<sup>a,b,†</sup>, Fan Yang<sup>a,‡</sup>, Jian-ping Wang<sup>a,\*</sup>*a. Beijing National Laboratory for Molecular Sciences, Molecular Reaction Dynamics Laboratory, Institute of Chemistry, Chinese Academy of Sciences, Beijing 100190, China**b. University of Chinese Academy of Sciences, Beijing 100049, China*

(Dated: Received on December 15, 2015; Accepted on January 13, 2016)

Vibrational and structural dynamics of two transition metal carbonyl complexes,  $\text{Mn}(\text{CO})_5\text{Br}$  and  $\text{Re}(\text{CO})_5\text{Br}$  were examined in DMSO, using ultrafast infrared pump-probe spectroscopy, steady-state linear infrared spectroscopy and quantum chemistry computations. Two carbonyl stretching vibrational modes (a low-frequency  $A_1$  mode and two high-frequency degenerate E modes) were used as vibrational probes. Central metal effect on the CO bond order and force constant was responsible for a larger E- $A_1$  frequency separation and a generally more red-shifted E and  $A_1$  peaks in the Re complex than in the Mn complex. A generally broader spectral width for the  $A_1$  mode than the E mode is believed to be partially due to vibrational lifetime effect. Vibrational mode-dependent diagonal anharmonicity was observed in transient infrared spectra, with a generally smaller anharmonicity found for the E mode in both the Mn and Re complexes.

**Key words:** Transition metal carbonyl, Transient IR spectroscopy, Vibrational relaxation, Anharmonicity

## I. INTRODUCTION

It is well known that transition metal carbonyl coordination compounds play a very critical role in catalyzing chemical reactions, however, it still remains as a challenge for chemists to uncover the fundamental mechanisms lying underneath the complicated catalytic processes [1]. Vibrational excited states, in particular those of carbonyl ligands, are very important in these catalytic reactions. Infrared (IR) spectroscopy, particularly ultrafast time-resolved IR spectroscopy, is a powerful tool to investigate complicated molecular structures and structural processes at the level of chemical-bond structural sensitivity and on the time scale of femtosecond temporal sensitivity [2–4]. Tabletop Ti:sapphire laser and optical parametric amplifier technologies can now generate stable femtosecond IR pulses, providing excellent light sources for ultrafast transient IR spectroscopic measurements. One of such measurements is pump-probe. In a typical IR pump-probe experiment, a relatively intense IR pulse (referred as pump) is used to excite a subensemble of a condensed-phase molecule (solute) to a specific vibra-

tional excited state, a weak IR pulse (referred as probe) is followed with a varying delay time to characterize the vibrational relaxations of the excited states. Because molecular vibrations are directly influenced by the molecular structures as well as by instantaneous solvent configurations, the IR pump-probe method provides a sensitive measurement of both vibrational relaxations and molecular structural dynamics. With the aid of femtosecond IR laser pulses, the time resolution of this method is readily comparable to that of molecular dynamics simulations.

Manganese and rhenium pentacarbonyl bromides ( $\text{Mn}(\text{CO})_5\text{Br}$  and  $\text{Re}(\text{CO})_5\text{Br}$ ) are typical transition metal carbonyl coordination compounds that can be used as model molecules to understand the vibrational properties of these transition metal carbonyl species. The two complexes share the same formula,  $\text{M}(\text{CO})_5\text{Br}$  ( $\text{M}=\text{Mn}$  and  $\text{Re}$  respectively), and have  $C_{4v}$  symmetry. In this work, we are particularly concerned with the carbonyl stretching mode ( $\nu_{\text{CO}}$ ) whose vibrational frequency is located in the 5- $\mu\text{m}$  wavelength region ( $2000\text{ cm}^{-1}$  in wavenumber). The vibrational representation of  $\text{M}(\text{CO})_5\text{Br}$  complexes contains two infrared-active  $\nu_{\text{CO}}$  modes ( $A_1$  and E) [5], which are mainly the axial and equatorial CO stretching vibrations respectively. While it has been established that the vibrational frequency of these two modes is in the order of  $E > A_1$ , the vibrational and structural dynamics underneath these two modes, and the influence of central metal atom on the vibrational dynamics, are less under-

<sup>†</sup>Part of the special issue for “the Chinese Chemical Society’s 14th National Chemical Dynamics Symposium”.

<sup>‡</sup>They contributed equally to this work.

\*Author to whom correspondence should be addressed. E-mail: jwang@iccas.ac.cn, Tel.:+86-10-62656806, FAX:+86-10-62563167

stood.

Further, the carbonyl stretching mode can be effectively used as a vibrational probe for the structures and dynamics of the transitional metal carbonyls [6]. The carbonyl stretching mode has a large transition dipole moment and an absorption linewidth that are sensitive to both molecular structure and solvent environment [7]. The carbonyl stretching mode also usually has a vibrational lifetime that falls into the picosecond time regime [8], providing a time window for examining the ultrafast structural dynamics of these transition metal compounds. An aprotic polar solvent, namely dimethyl sulfoxide (DMSO), was selected in this work because it can dissolve manganese and rhenium pentacarbonyl bromides at reasonable concentration, also because it is relevant in catalytic and photophysical studies.

## II. MATERIALS AND METHODS

### A. Sample and FTIR experiments

Mn(CO)<sub>5</sub>Br and Re(CO)<sub>5</sub>Br were purchased from Sigma-Aldrich and used without further purification. The two transition metal carbonyl complexes were dissolved in DMSO at concentrations of 10.8 and 17.1 mmol/L, respectively. The sample solutions were loaded into a home-made liquid IR sample-cell, which is composed of two 2-mm thick calcium fluoride windows and separated by a 50- $\mu$ m thick Teflon spacer. FTIR spectra were collected using a Nicolet 6700 FTIR spectrometer (Thermo Electron) at 1-cm<sup>-1</sup> spectral resolution. The FTIR experiments were carried out at room temperature (22 °C).

### B. Pump-probe spectroscopy

The transient IR pump-probe experiments were carried out with a home-built IR pump-probe spectrometer [9, 10]. Mid-infrared pulses with central frequency at near 2000 cm<sup>-1</sup> were generated via a difference frequency generator (DFG) that was pumped by an optical parametric amplifier (OPA), and the latter was pumped by a Ti:sapphire laser amplifier system (sub 35-fs pulse width, 800-nm central wavelength, and 1-kHz repetition rate). The pump and probe pulses were generated by a beam splitter subsequently collimated and focused on the sample cell by a focusing parabolic mirror with 10-cm focal length. The time delay between the pump and probe pulses was controlled with a motorized translation stage. The polarization direction of the probe pulse, with respect to that of the pump pulse, was adjusted to 54.7° (the so-called “magic” angle [11]) via a half-wave plate and a polarizer, at which angle the lifetime of the vibrational excited state can be measured free from molecular reorientational effects.

Transient spectra were obtained by chopping the

pump pulse at half of the laser repetition. Sample position was controlled with a manual mechanical XYZ-translation stage. The nonlinear IR experiments were carried out at room temperature (22 °C).

### C. Quantum chemistry calculation

Geometry optimization of both Mn(CO)<sub>5</sub>Br and Re(CO)<sub>5</sub>Br was carried out and followed by subsequent vibrational frequency analysis including anharmonicity computations, in implicit solvent using polarizable continuum model (PCM) [12, 13] with default parameters for DMSO. Density functional (B3LYP) with the 6-31++G\*\* basis set for light atoms (C, O, and Br) and the Lanl2dz pseudopotential for the central transition metal atom were used. All computations were performed using the density functional theory (DFT) as implemented in Gaussian 09 [14].

## III. RESULTS AND DISCUSSION

### A. Linear IR spectra

The infrared spectra of Mn(CO)<sub>5</sub>Br and Re(CO)<sub>5</sub>Br dissolved in DMSO in the CO stretching region are shown in Fig.1 with peak intensity normalized. Clearly, for each compound, five CO groups exhibit only two absorption peaks, and show compound-dependent peak positions and peak separations. The bands from the high- to low-frequency direction are denoted as two infrared-active  $\nu_{\text{CO}}$  modes (E and A<sub>1</sub>) respectively by symmetry coordinate [5], which are mainly the axial and equatorial CO stretching vibrations respectively. It is noticed that the E mode is a doubly degenerate mode with identical frequency. This is verified by DFT computations (see below).

Table I is the fitting result of the experimental IR spectra using Voigt function. The Voigt function is used because neither pure Gaussian nor pure Lorentzian function could yield a satisfactory fitting result. Peak widths are reported in the form of full-width at half-maximum (FWHM), showing a tendency of increase as the metal center changes from manganese to rhenium. In addition, for the same molecule, the FWHM for the E mode is generally narrower than that for the A<sub>1</sub> mode, whose significance will be explained in later section.

### B. Computations

To understand the observed IR spectra and vibrational frequency change associated with central atom, we performed quantum chemistry calculations on each complex in implicit DMSO solvent using the PCM method. Figure 2 shows the two optimized structures

TABLE I Voigt function fitting parameters of the linear IR spectra of the CO stretching of  $\text{Mn}(\text{CO})_5\text{Br}$  and  $\text{Re}(\text{CO})_5\text{Br}$  dissolved in DMSO.

	Mode	Peak <sup>a</sup>	FWHM <sup>a</sup>	Area <sup>b</sup>
$\text{Mn}(\text{CO})_5\text{Br}$	E	2043.7	20.4	24.6
	$A_1$	2009.0	27.4	7.7
$\text{Re}(\text{CO})_5\text{Br}$	E	2037.6	23.5	29.4
	$A_1$	1984.7	31.4	9.9

<sup>a</sup> Peak position and FWHM are in unit of  $\text{cm}^{-1}$ .

<sup>b</sup> Area is in unit of arbitrary unit.

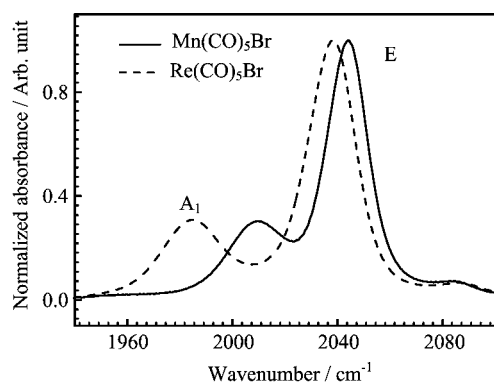


FIG. 1 Linear IR spectra of  $\text{Mn}(\text{CO})_5\text{Br}$  and  $\text{Re}(\text{CO})_5\text{Br}$  dissolved in DMSO in the CO stretching region. The bands from low frequency to high frequency in DMSO are denoted as  $A_1$  and E.

with key bond distances listed, each showing a  $C_{4v}$  symmetry with relatively elongated CO bond length in the case of  $\text{Re}(\text{CO})_5\text{Br}$ . Table II lists the computed vibrational parameters. In Table II, the IR active  $A_1$  and doubly degenerate E modes are predicted. Normal-mode analysis shows that the E mode is mainly due to four radial CO stretching vibrations, while the  $A_1$  mode is mainly due to the single axial CO stretching. This is in agreement with previous assignment [5]. The computation not only reproduces experimentally observed order for the E and  $A_1$  modes in both frequency and intensity in each complex, but also reproduces the frequency shift as a function of metal center mainly in two aspects: first, as metal center goes from Mn to Re, both vibrational modes are red shifted (*i.e.* towards the low-frequency side); second, the E and  $A_1$  frequency separation becomes larger as metal center goes from Mn to Re. Because the two complexes are believed to have identical molecular symmetry ( $C_{4v}$ ) [15], these changes are attributed to the effect of the central atom, which both belong to the VIIB group in the Periodic Table of element.

For carbonyl metal complexes, the intense carbonyl stretching bands are known to be closely related to back bonding effects [16] that result from the interaction between the unoccupied antibonding ( $\pi^*$ ) orbitals of the

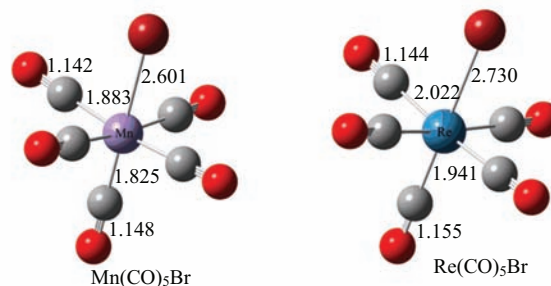


FIG. 2 Molecular structure of  $\text{Mn}(\text{CO})_5\text{Br}$  and  $\text{Re}(\text{CO})_5\text{Br}$  with  $C_{4v}$  symmetry. These important bond lengths are marked

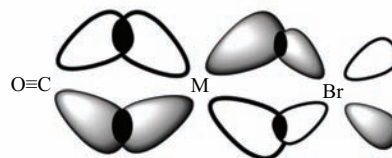


FIG. 3 Carbon monoxide ligand acts as a strong acceptor in  $\text{Mn}(\text{CO})_5\text{Br}$  and  $\text{Re}(\text{CO})_5\text{Br}$  complexes. Only the axial direction is shown.

TABLE II Calculated CO stretching vibration frequency  $\nu$ , reduced mass  $\mu$ , force constant  $k$  (in unit of  $\text{mDyne}/\text{\AA}$ ), transition intensity  $I$  for the  $A_1$  and E modes in  $\text{Mn}(\text{CO})_5\text{Br}$  and  $\text{Re}(\text{CO})_5\text{Br}$ .

	Mode	$\nu/\text{cm}^{-1}$	$\mu/\text{amu}$	$k$	$I/(\text{km}/\text{mol})$
$\text{Mn}(\text{CO})_5\text{Br}$	$A_1$	2076.2	13.39	34.02	1328.4
	E	2103.9	13.44	35.05	2323.9
$\text{Re}(\text{CO})_5\text{Br}$	$A_1$	2032.3	13.35	32.49	1875.8
	E	2078.9	13.45	34.25	3187.9

carbonyl group and the d orbital electrons of the metal center. This is illustrated in Fig.3. Further, because the d orbital electron energy in Re is lower than that in Mn, a better energy match with the energy of the  $\pi^*$  orbitals of the carbonyl ligand in the case of Re is expected, thus forming stronger back bonding. Such a stronger back bonding also causes a Re–C bond length shortening in comparison with a single ReCO case (not given here). This causes C atom to be less positively charged and thus weakens the CO bond strength (decreases its bond order) and generally increases its bond length (Fig.2), resulting in a lowered vibrational frequency in the  $\text{Re}(\text{CO})_5\text{Br}$  complex than that in the  $\text{Mn}(\text{CO})_5\text{Br}$  complex. Because the four equatorial CO share the d orbital interaction, a rather limited red shift in frequency is expected for the E mode in the Re complex with respect to that in the Mn complex. This is the reason for larger E- $A_1$  frequency separation in the Re complex.

Further, Table II suggests that the metal atom effect is mainly reflected in the force constant of the carbonyl stretch. Figure 4 shows the relationship between the computed frequency and the square root of the force constant for the E and  $A_1$  modes in two transition metal

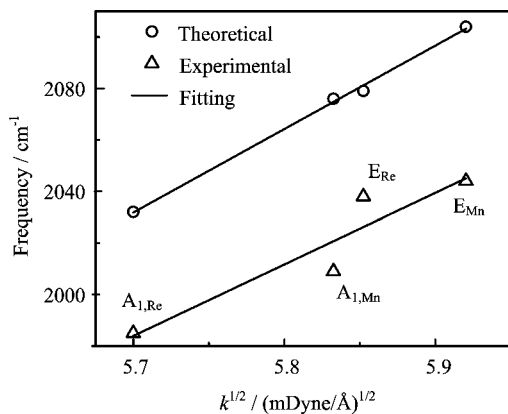


FIG. 4 Theoretically computed frequency versus force constant for the CO stretching modes of  $\text{Mn}(\text{CO})_5\text{Br}$  and  $\text{Re}(\text{CO})_5\text{Br}$ . Experimentally observed frequencies are also plotted.

complexes, which is indeed more or less linearly correlated as predicted. The experimental frequencies are also plotted for a direct comparison, in which a linear fitting also seems reasonable. On the other hand, it should be pointed out that the reduced mass is also a factor because the frequency is proportional to  $\mu^{-1/2}$ . However, from the  $A_1$  mode to E mode, their frequencies are not proportional to  $\mu^{-1/2}$ , because the two modes have slightly different  $\mu$  values. In addition, the CO bond lengths also generally increase in  $\text{Re}(\text{CO})_5\text{Br}$  as shown in Fig.2, which is the result of stronger back bonding. The increased bond length is apparently proportional to the increased frequency as well.

### C. Pump-probe spectroscopy

The pump-probe spectra of both  $\text{Mn}(\text{CO})_5\text{Br}$  and  $\text{Re}(\text{CO})_5\text{Br}$  were obtained in the CO stretching vibration frequency region, of which the results are shown in Fig.5. This contour plot maps the state evolution of the vibrationally excited carbonyl stretching as a function of the pump-probe delay time. The magic-angle polarization condition is chosen so that the molecular orientational effect is removed and only true vibrational relaxation can be seen. Here for simplification the zero delay time is set to when maximum pump-probe signal was observed, and instrumental response function deconvolution was not carried out. Nevertheless, the lifetime evaluation, which is found to be tens of picosecond (see below), will not be significantly affected by the inclusion of the instrumental response function. Two types of signals corresponding to a given peak in the linear IR (*e.g.* the E mode), are shown as a negative signal (plotted in blue color) due to vibrational-state bleaching and stimulated emission (from  $v=0$  to  $v=1$ , where  $v$  is vibrational quantum number), and as a positive signal (plotted in red color) due to the first excited state

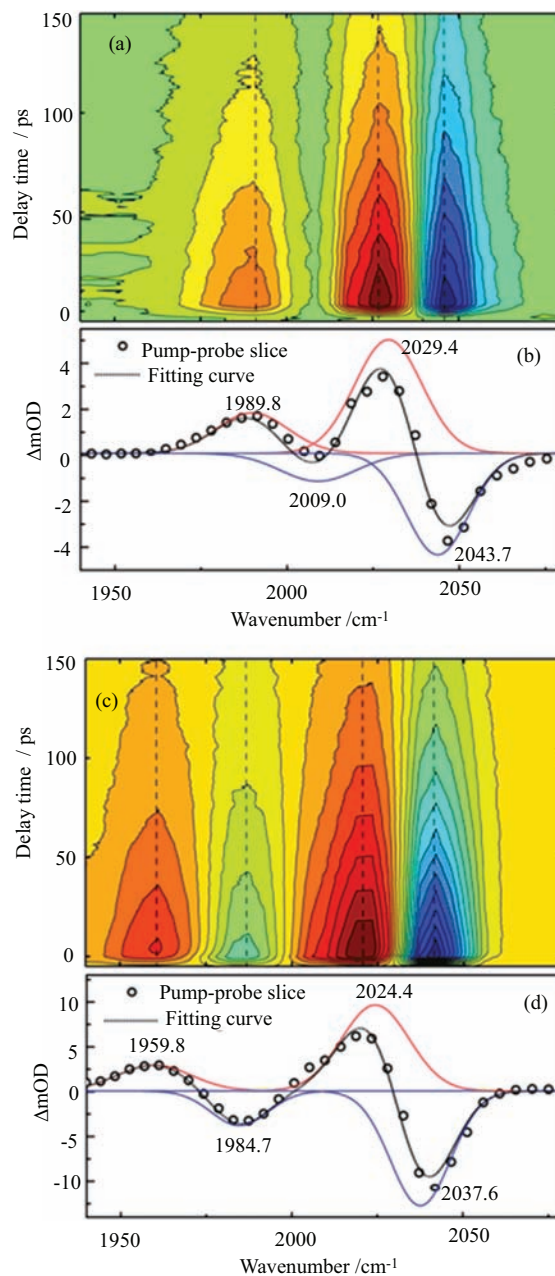


FIG. 5 Magic-angle pump-probe spectra of (a)  $\text{Mn}(\text{CO})_5\text{Br}$  and (c)  $\text{Re}(\text{CO})_5\text{Br}$  in the CO stretching region. Decomposition of transient spectra at 0 fs delay time of (b)  $\text{Mn}(\text{CO})_5\text{Br}$  and (d)  $\text{Re}(\text{CO})_5\text{Br}$  for anharmonicity evaluation.

absorption (from  $v=1$  to  $v=2$ ). The red and blue signals are separated in the frequency range shown in Fig.5 due to vibrational anharmonicity ( $\Delta = \delta E_{0-1} - \delta E_{1-2}$ , where  $\delta E$  is corresponding two-level vibrational energy separation).

The E and  $A_1$  modes are more separated in frequency for the Re complex than for the Mn complex, so that the absorption and bleach signals are clearly shown in the former but not in the latter. Note that ground-state bleaching signal of  $\text{Mn}(\text{CO})_5\text{Br}$  in the  $A_1$  mode appears

TABLE III Vibrational lifetime ( $T_1$ ) obtained by single exponential fitting the magic-angle data for the Mn(CO)<sub>5</sub>Br and Re(CO)<sub>5</sub>Br complexes at desired frequency positions: bleaching ( $\nu_{0\rightarrow 1}$ ) and absorption ( $\nu_{1\rightarrow 2}$ ).

Solute	$\nu/\text{cm}^{-1}$	Assignment	$T_1/\text{ps}$
Mn(CO) <sub>5</sub> Br	1991	$\nu_{1\rightarrow 2}$ , A <sub>1</sub>	87.7±0.4
	2027	$\nu_{1\rightarrow 2}$ , E	102.8±0.7
	2046	$\nu_{0\rightarrow 1}$ , E	100.8±0.3
Re(CO) <sub>5</sub> Br	1963	$\nu_{1\rightarrow 2}$ , A <sub>1</sub>	81.3±0.5
	1985	$\nu_{0\rightarrow 1}$ , A <sub>1</sub>	77.0±1.0
	2017	$\nu_{1\rightarrow 2}$ , E	93.6±0.8
	2040	$\nu_{0\rightarrow 1}$ , E	86.4±0.5

to be missing in Fig.5(a) due to signal overlap between the 0-1 and 1-2 transitions. This missing spectral component can be identified by spectral fitting (Fig.5(b)).

To have a detailed understanding of the ultrafast dynamics in relative to those vibrational transitions investigated, we extracted the temporal evolution of the population distribution at the maximum intensity of the excited state transitions, which are shown in Fig.6 for the Mn(CO)<sub>5</sub>Br and Re(CO)<sub>5</sub>Br complexes. These vibrational relaxation traces were fitted reasonably by single exponential decay, of which parameters are summarized in Table III.

One may intuitively think that those two complexes should have the same vibrational relaxation behavior for their very much alike molecular structure. However, our experiment results show that there is a significant difference between the  $T_1$  times for the E and A<sub>1</sub> modes in a given transition metal complex, and there is also some dependence on the transition metal center. Specifically, for the Mn complex, the  $T_1$  time of the A<sub>1</sub> mode (87.7 ps) is nearly 10% faster than the E mode (ca. 101 ps). For the Re complex, the  $T_1$  time of the A<sub>1</sub> mode (ca. 80 ps, averaged from  $v=0$  to  $v=1$  and  $v=1$  to  $v=2$  transitions) is also nearly 10% faster than the E mode (ca. 90 ps, averaged from  $v=0$  to  $v=1$  and  $v=1$  to  $v=2$  transitions).

These  $T_1$  values are found to roughly anticorrelate with the behavior of the linewidth shown in the linear IR spectra (Fig.1), that is, the shorter the  $T_1$ , the broader the spectral width, which is found to be true for both Mn and Re complexes. In addition, the linewidth in the E and A<sub>1</sub> modes are generally broader in the Re complex than in Mn complex, which is also in agreement with relatively shorter  $T_1$  observed in the Re complex than in Mn complex. Of course, the discussion here simply ignores the contribution of inhomogeneous broadening. The question is why the A<sub>1</sub> mode is nearly 10% shorter lived than the E mode? It could be due to a better energy match between the A<sub>1</sub> mode and linear combinations of low-frequency solvent modes; it could be also due to the axial bromide ligand effect. Even though the data are solid, a definite answer cannot be

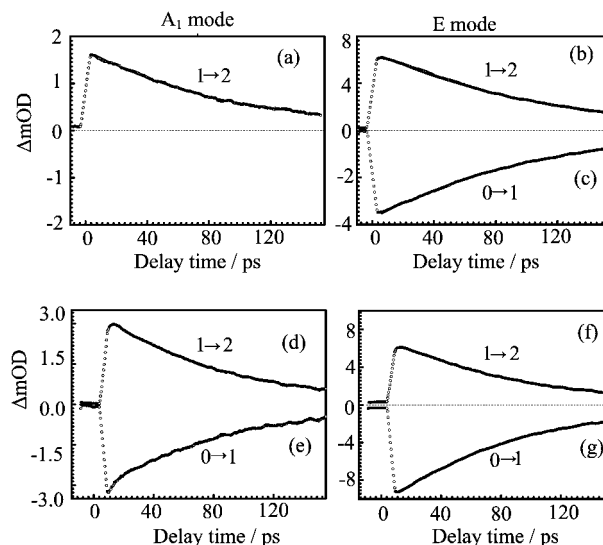


FIG. 6 Population relaxation dynamics of the CO stretching mode of (a, b, and c) Mn(CO)<sub>5</sub>Br and (d, e, f, and g) Re(CO)<sub>5</sub>Br. Experimental data (circle) and exponential fitting (solid line) are given. Probing frequency positions are marked as dashed lines in Fig.5 (a) and (c).

provided at this moment.

#### D. Anharmonicity

In Fig.5 the contour plot clearly shows the presence of anharmonicity for both the E and A<sub>1</sub> modes in the two transition metal carbonyls. By taking a slice of the time-dependent transient absorption spectra at a given delay time, the anharmonicity of each mode can be extracted. Early-time spectra were used to avoid cross-peak contributions due to intramolecular vibrational redistribution that may occur at longer time [17]. The results are shown in Fig.5 (b) and (d). Here the diagonal anharmonicity for a given mode is measured, which is defined as  $\Delta = \delta E_{0-1} - \delta E_{1-2}$ , as mentioned above. For each transient spectrum, two pairs of Gaussian functions were utilized (for simplification) with negative peak positions fixed to those observed in the linear IR spectra (Fig.1). For the E mode the anharmonicity was determined to be 14.3 cm<sup>-1</sup>, while for the A<sub>1</sub> mode the anharmonicity was 17.7 cm<sup>-1</sup>. For the Re complex, the anharmonicity of the E and A<sub>1</sub> mode was determined to be 13.3 and 24.9 cm<sup>-1</sup>, respectively.

To evaluate the diagonal anharmonicity of the carbonyl stretching modes in the two transition metal complex, *ab initio* computations were carried out using the method outlined in previous work [18, 19]. It was found that for both the Mn and Re complexes, the diagonal anharmonicity of the E mode is generally smaller than that of the A<sub>1</sub> mode (data not shown), which is in general agreement with the experimental results.

These results show that due to the nature of the

vibrational mode ( $A_1$  mode is mainly the axial CO stretching vibration while the degenerate E modes are mainly the linear combination of the four equatorial CO stretching vibrations), the diagonal anharmonicity of the E modes is generally smaller than that of the  $A_1$  mode. This is understandable because more delocalized modes tend to smaller diagonal anharmonicity [19], which is the case of E mode in the present work. No obvious metal center dependence can be obtained, either due to the limitation of the spectral-resolution of the pump-probe method in measuring the anharmonicity, or due to the possibility that the metal-center dependence on the carbonyl stretching anharmonicity is insignificant for the two cases studied here. At the moment, our data cannot differentiate these two possibilities.

#### IV. CONCLUSION

In this work, we investigated two typical transition metal carbonyl coordination compounds which have different central metal atoms, namely  $Mn(CO)_5Br$  and  $Re(CO)_5Br$ . Examination of the carbonyl stretching modes of the two compounds in an aprotic but polar solvent (DMSO) using steady-state linear infrared and time-resolved nonlinear infrared methods yields detailed insights into the structural and vibrational relaxation dynamics of the two carbonyl complexes in solution phase. From Mn to Re, the metal center dependent linear IR feature is seen and explained as the  $\pi$  backbonding effect, which results in a larger E- $A_1$  mode vibrational frequency separation and a generally red-shifted E and  $A_1$  modes in the case of Re. A generally broader spectral width for the low-frequency  $A_1$  mode than the high-frequency E mode is believed to be partially due to the vibrational lifetime ( $T_1$ ) effect. By ignoring the inhomogeneous broadening contribution, the  $T_1$  time is shorter for the  $A_1$  mode, whose spectral width (FWHM) is also broader, due to the well-known  $1/2T_1$  contribution to the total spectral linewidth [2]. This is found to be true in both Mn and Re complexes. Finally vibrational diagonal anharmonicity for the E and  $A_1$  modes are measured from the early-time transient pump-probe spectra. The anharmonicity of the E mode is found to be generally smaller in both Mn and Re complexes, which is believed to be associated with the more delocalized nature of the E mode. These results provide fundamental measurements of the vibrational signatures of the VIIB-group transition metal carbonyl complexes.

#### V. ACKNOWLEDGMENTS

This work was supported by the Hundred Talent Fund of the Chinese Academy of Sciences, and also sup-

ported by the National Natural Science Foundation of China (No.21473212, No.20727001 and No.21573243). The author thanks P. Yu and J. Zhao for their technical assistances.

- [1] M. Chergui, *Acc. Chem. Res.* **48**, 801 (2015).
- [2] J. C. Owrutsky, D. Raftery, and R. M. Hochstrasser, *Annu. Rev. Phys. Chem.* **45**, 519 (1994).
- [3] M. D. Fayer, *Annu. Rev. Phys. Chem.* **21** (2009).
- [4] L. M. Kiefer, J. T. King, and K. J. Kubarych, *Acc. Chem. Res.* **48**, 1123 (2015).
- [5] D. Kariuki and S. F. A. Kettle, *Spectrochim. Acta A* **34**, 563 (1978).
- [6] J. K. McCusker, *Acc. Chem. Res.* **36**, 876 (2003).
- [7] E. J. Heilweil, R. R. Cavanagh, and J. C. Stephenson, *Chem. Phys. Lett.* **134**, 181 (1987).
- [8] E. J. Heilweil, R. R. Cavanagh, and J. C. Stephenson, *J. Chem. Phys.* **89**, 230 (1988).
- [9] D. Li, F. Yang, C. Han, J. Zhao, and J. Wang, *J. Phys. Chem. Lett.* **3**, 3665 (2012).
- [10] F. Yang, P. Yu, J. Zhao, and J. Wang, *ChemPhysChem* **14**, 2497 (2013).
- [11] G. Fleming, *Chemical Applications of Ultrafast Spectroscopy*, 1st Edn., Oxford: Oxford University Press (1986).
- [12] E. Cancès, B. Mennucci, and J. Tomasi, *J. Chem. Phys.* **107**, 3032 (1997).
- [13] B. Mennucci and J. Tomasi, *J. Chem. Phys.* **106**, 5151 (1997).
- [14] M. J. Frisch, G. W. Trucks, H. B. Schlegel, G. E. Scuseria, M. A. Robb, J. R. Cheeseman, G. Scalmani, V. Barone, B. Mennucci, G. A. Petersson, H. Nakatsuji, M. Caricato, X. Li, H. P. Hratchian, A. F. Izmaylov, J. Bloino, G. Zheng, J. L. Sonnenberg, M. Hada, M. Ehara, K. Toyota, R. Fukuda, J. Hasegawa, M. Ishida, T. Nakajima, Y. Honda, O. Kitao, H. Nakai, T. Vreven, J. A. Montgomery Jr., J. E. Peralta, F. Ogliaro, M. Bearpark, J. J. Heyd, E. Brothers, K. N. Kudin, V. N. Staroverov, R. Kobayashi, J. Normand, K. Raghavachari, A. Rendell, J. C. Burant, S. S. Iyengar, J. Tomasi, M. Cossi, N. Rega, J. M. Millam, M. Klene, J. E. Knox, J. B. Cross, V. Bakken, C. Adamo, J. Jaramillo, R. Gomperts, R. E. Stratmann, O. Yazyev, A. J. Austin, R. Cammi, C. Pomelli, J. W. Ochterski, R. L. Martin, K. Morokuma, V. G. Zakrzewski, G. A. Voth, P. Salvador, J. J. Dannenberg, S. Dapprich, A. D. Daniels, Ö. Farkas, J. B. Foresman, J. V. Ortiz, J. Cioslowski and D. J. Fox, *Gaussian 09*, Revision A.02, Wallingford, CT: Gaussian Inc., (2009).
- [15] Y. F. Hu, G. M. Bancroft, and K. H. Tan, *Inorg. Chem.* **39**, 1255 (2000).
- [16] G. L. Miessler, P. J. Fischer, and D. A. Tarr, *Inorganic Chemistry*, 5th Edn., New Jersey: Pearson (2013).
- [17] F. Yang, P. Yu, J. Zhao, J. Shi, and J. Wang, *Phys. Chem. Chem. Phys.* **17**, 14542 (2015).
- [18] V. Barone, *J. Chem. Phys.* **122**, 014108/1 (2005).
- [19] J. Wang and R. M. Hochstrasser, *J. Phys. Chem. B* **110**, 3798 (2006).